ELSEVIER

Journal of Magnetism and Magnetic Materials 170 (1997) 110–128

journal of magnetism and magnetic materials

Evidence for biquadratic exchange interactions in $GdAg_{1-x}Zn_x$

U. Köbler[a,*], J. Schweizer[b], P. Chieux[b], Th. Lorenz[c], B. Büchner[c], W. Schnelle[d], F. Deloie[a], W. Zinn[a]

[a] *Institut für Festkörperforschung, KFA Jülich, D-52425 Jülich, Germany*
[b] *Institut Laue-Langevin, F-38042 Grenoble, France*
[c] *II. Physikalisches Institut, Universität zu Köln, D-50937 Köln, Germany*
[d] *Max-Planck-Institut für Festkörperforschung, D-70569 Stuttgart, Germany*

Received 23 September 1996

Abstract

We have re-examined the magnetic-phase diagram of $GdAg_{1-x}Zn_x$, an intermetallic solid solution of a ferromagnet (GdZn) and an antiferromagnet (GdAg). Samples of the intermediate composition range $0.48 < x < 0.59$ show new magnetic-ordering phenomena and all exhibit nearly the same phase diagram at the application of a magnetic field. These phase diagrams comprise two ferrimagnetic phases with ground-state magnetization values of $m \approx \frac{1}{3}$ and $m \approx \frac{2}{3}$ and one uncommon high-temperature phase which is nearly ferromagnetic but which has a finite susceptibility and therefore no spontaneous magnetization. All ordered phases seem to coexist at one multicritical point. It is argued that the observed variety of magnetic phases is due to biquadratic exchange interactions which remain as the only active ones in a situation where the ferromagnetic and antiferromagnetic bilinear interactions compensate each other. The easiest method to identify biquadratic interactions is the Curie–Weiss law of the cubic susceptibility χ_3. However, in metallic systems the Curie–Weiss temperature regime of χ_3 is not nearly reached even at five times the ordering temperature, thus preventing the evaluation of θ_3 which provides a measure for the strength of the biquadratic interaction in insulating systems. This shows that there are much stronger and strongly temperature-dependent individual biquadratic interaction processes of either sign than one might assume according to the macroscopically observed average interaction. Although the existence of the new magnetically ordered states is confirmed with magnetization, dilatometric and specific heat measurements, no corresponding neutron-diffraction intensities are observed in zero-magnetic field which points to strongly fluctuating or non-collinear magnetic structures. Since the outlined observations fall into a composition and temperature range in this random magnetic-bond system where magnetic non-equilibrium phenomena become visible, special precautions are necessary to obtain the low-temperature equilibrium magnetization curves.

Keywords: Biquadratic exchange; Magnetic metals; Magnetic phases

1. Introduction

In a recent publication it has been shown that, in EuSe and EuTe, biquadratic three and four spin-exchange interactions of the type $(S_1 \cdot S_2)^2$,

* Corresponding author. Fax: + 49 246 167 2076.

PII S0304-8853(96)00007-3

$(S_1 \cdot S_2)(S_2 \cdot S_3)$ and $(S_1 \cdot S_2)(S_3 \cdot S_4)$ contribute appreciably to the total magnetic interaction [1]. As a qualitative explanation for the importance of those interactions (which for simplicity will be called biquadratic in the following) one may argue that in both compounds the effective bilinear interaction is weak due to the fact that positive nearest and negative next-nearest neighbour interactions compensate [2] and this increases the weight of biquadratic interactions. As a consequence, the heuristic rule may be given that magnetic materials with a noticeable content on biquadratic interaction are to be seeked among those with low ordering temperatures. Little is known about the relative strength of bilinear and biquadratic interactions. In Ref. [1] it could be shown that for all europium monochalcogenides the total biquadratic interaction is ferromagnetic while the total bilinear interaction changes from ferromagnetic for EuO to antiferromagnetic for EuTe [2]. Since many different processes with positive and negative coupling constants contribute to the total biquadratic interaction, a conflicting situation between some of them and the leading bilinear interaction may be given such that thermodynamic non-equilibrium phenomena may result in magnetization measurements. For instance, by diluting EuTe with the isomorphic diamagnetic material SrTe it could be verified that in this antiferromagnetic solid solution series biquadratic interactions are antiferromagnetic but three-spin interactions are ferromagnetic [3]. Therefore, if thermodynamic non-equilibrium phenomena are observed in a homogeneous system like GdAg they may constitute a fingerprint of an underlying biquadratic interaction opposite in sign to the dominating bilinear interaction which defines the magnetic order.

By means of alloying a ferromagnet like GdZn ($T_c = 269$ K) and an antiferromagnet like GdAg ($T_N = 136$ K) a compensation between ferromagnetic and antiferromagnetic interactions can be achieved and this should increase the importance of biquadratic interactions. This idea seems to hold for $GdAg_{1-x}Zn_x$. In an earlier publication [4] it has been reported that in this CsCl-type ternary alloy system a new magnetic phase with a spontaneous saturation magnetization of $m_s \approx \frac{1}{3}$ exists in the intermediate composition range $0.48 < x < 0.59$. Such a phase with a first-order transition is not to be expected if only bilinear interactions were present.

Here we will show mainly with magnetostriction measurements that this is not the only novel ordered phase but that a rather composition-independent complex magnetic phase diagram pertains to all samples with $0.48 < x < 0.59$. In particular, the composition independence of the first-order phase transition into the ferrimagnetic phase labelled ferri I at ≈ 25 K supports the idea that this ordering phenomenon is due to another type of interaction which changes in the range $0.48 < x < 0.59$ much less with composition than the bilinear exchange interaction. First-order transitions as a consequence of a sufficiently strong content on biquadratic interaction have been predicted [5–7] and EuSe seems to be another realization for this possibility [1, 8, 9].

A quantitative measure for the biquadratic interaction strength is given by the Curie–Weiss temperature θ_3 of the cubic susceptibility χ_3 defined by Eq. (1) below. This method of evaluation worked excellently in the case of the insulating europium monochalcogenides [1], but in metallic systems the Curie–Weiss regime of χ_3 is not reached even at temperatures larger than ten times the ordering temperature which, as a consequence, requires a high experimental precision in order to measure the associated small χ_3 values reliably. The behaviour of χ_3 is in contrast to that one of the linear susceptibility χ_1 which approaches the Curie–Weiss law in a satisfactory way for temperatures larger than only two times the ordering temperature.

One further unusual property of the cubic susceptibility observed here is that – depending on temperature – χ_3 can be larger (more ferromagnetic) or smaller (more antiferromagnetic) compared to the calculated Curie law of χ_3 as it should apply for the situation without biquadratic interactions ($\theta_3 = 0$). Such a rapid alternation is not known for the linear susceptibility χ_1, which is either entirely larger or smaller than the calculated Curie susceptibility with $\theta_1 = 0$. This strange behaviour of the cubic susceptibility points to rather strong individual biquadratic interaction processes which apparently have different signs and nearly compensate each other such that the cubic susceptibility $\chi_3(T)$ reveals only some weighted average of

the different temperature dependences of all particular biquadratic interaction processes. Evidently, the temperature dependence of the cubic susceptibility contains useful information on the band structure and is worthy of investigation in more detail with theoretical and experimental methods, but those aspects are outside the scope of this work.

A ferrimagnetically ordered state with a spontaneous magnetization of $\frac{1}{3}$ as observed in $GdAg_{1-x}Zn_x$ for $0.48 < x < 0.59$ is also known for EuSe [1, 8] and EuC_6 [11], which are two other materials in which strong biquadratic interactions have been identified. In both materials, the associated magnetic structures have not been resolved unambiguously, although an elaborate neutron scattering study exists for EuSe [10]. In the case of EuC_6 a magnetic structure model has been proposed but this was not verified by a microscopic method such as neutron scattering. It is very surprising that a ferrimagnetic state with a spontaneous magnetization of $m_s \approx \frac{1}{3}$ is found on so very different magnetic lattices. For EuSe the magnetic sublattice is FCC, for EuC_6 HCP and for $GdAg_{1-x}Zn_x$ simple cubic. It is especially difficult to imagine a ferrimagnetic order on a simple cubic lattice occupied with equivalent magnetic moments. On the other hand, molecular field investigations of this problem have shown that the effects induced by biquadratic interactions do not depend much on the symmetry properties of the magnetic lattice [6].

In resolving the magnetic structure of mixed crystals with biquadratic interactions by means of neutron scattering it is very important to consider the absolute scattering intensities as they can be obtained by a calibration against the observed nuclear scattering intensities. Such an analysis revealed that in $Eu_xSr_{1-x}Te$ the observed MnO superstructure reflection intensities are too weak and show the general tendency to decrease further with dilution, possibly because of broken three- and four-spin interactions [3]. The reduced MnO scattering intensities indicate fluctuating or non-collinear ordering structures which are difficult to distinguish from each other with scattering methods. Those effects can be very pronounced such that scattering methods may become ineffective or even useless. This seems to apply in a dramatic way for the metallic random bond system $GdAg_{1-x}Zn_x$ since no additional neutron scattering intensities could be observed for the novel magnetic phases in zero-field measurements, a result which can only be understood assuming fluctuating or non-collinear types of magnetic order. Hence, in the present study, the identification of the ordered states rests on dilatomeric, magnetization and specific heat measurements.

2. Sample preparation and characterization

Due to the high vapour pressure of Zn samples have been prepared as in Ref. [4] in closed Molybdenum crucibles sealed by electron-beam welding. Stoichiometric charges were heated to above the melting point of 1030°C and slowly cooled down to ambient temperature using rates of 10°/h near to the solidification point. Samples obtained in this way occasionally contained smaller amounts of foreign phases even though standard X-ray diffraction analyses revealed only CsCl lines which fulfilled the Vegard linear lattice parameter variation very well, as can be seen in Fig. 1. This result indicates that fairly homogeneous mixtures are obtained.

The presence of smaller traces of foreign phases became evident with magnetization measurements

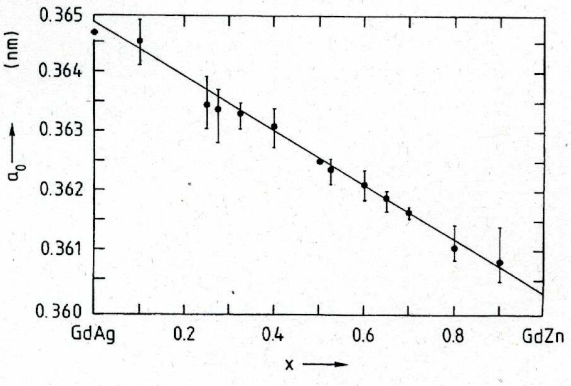

Fig. 1. Lattice parameter $a_0(x)$ of $GdAg_{1-x}Zn_x$ samples as determined by standard X-ray diffraction methods. The linear x-dependence (Vegard rule) indicates miscibility of both CsCl-type constituents.

on GdAg. For an isotropic or polycrystalline antiferromagnetic material the ratio between the susceptibility value at T_N, $\chi(T_N)$, and that for $T \to 0$, $\chi(0)$, should conform to $\chi(T_N)/\chi(0) = \frac{2}{3}$. This was however not observed for any of the repeated GdAg preparations. In contrast, mostly $\chi(0) > \chi(T_N)$ was found. Susceptibility measurements in different magnetic fields as displayed in Fig. 2 gave an explanation for this behaviour. The experimental data shown in Fig. 2 were only slightly shifted along the ordinate in order to become normalized at the Néel temperature of GdAg of $T_N = 136$ K. As can be seen, a strong non-linear field dependence occurs below a well-defined temperature of 115 K. This is attributed to a ferromagnetic component with a Curie temperature of 115 K. Since the magnetization of GdAg increases in a nearly linear way until the largest applied magnetic fields but the magnetization of the ferromagnetic foreign phase saturates, its importance on the total susceptibility gets consecutively weaker with increasing field. We were not able to identify the composition of this ferromagnetic precipitation, but it is evident that not only GdAg has been formed but also at least one further composition of the type Gd_nAg_m with unknown integers n and m. For a discussion of the known binary rare-earth alloys we refer the reader to Ref. [13]. Here, we restrict to mentioning that the content of this ferromagnetic component can be estimated to be less than 2%. It is clear that an antiferromagnetic precipitation in a ferromagnetic matrix contributes much less to the total susceptibility than vice versa.

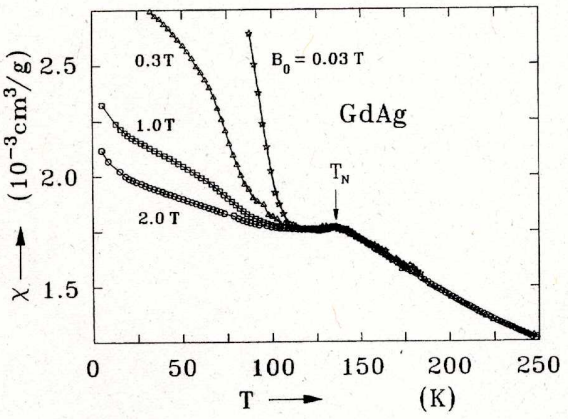

Fig. 2. Temperature dependence of magnetic susceptibility of GdAg measured in different external fields. The strong field dependence below about 115 K is attributed to a ferromagnetic precipitation which can be estimated to have a proportion of about 2%.

The just outlined compositional problems make clear that magnetization measurements may exhibit artefacts which should not be interpreted as an intrinsic property of the $GdAg_{1-x}Zn_x$ system such as a magnetic phase transition. On the other hand, genuine magnetic phase transitions driven by biquadratic exchange interactions are often associated with only minute magnetization anomalies and therefore a considerable ambiguity in the correct interpretation of the observed phenomena may be given. Here comparison with other experimental methods such as magnetostriction measurements can be very illuminative.

In the system $GdA_{1-x}Zn_x$ magnetoelastic effects are very pronounced and distinctive magnetostriction is observed at any magnetic phase transition, as will be shown below. Dilatometric measurements therefore provide a very efficient method to identify magnetic phase transitions and greatly help in the construction of the magnetic phase diagrams.

The following discussion of the complex magnetic phase diagram as it pertains to the samples with $0.48 < x < 0.59$ is therefore confined to those anomalies which are observed in measurements of the magnetostriction and the magnetization as well and which, as a consequence, can confidently be viewed as magnetic phase transitions.

One further quantity able to characterize the quality of the samples is the composition dependence of the Curie–Weiss temperature of the linear susceptibility $\theta_1(x)$ which is shown in the upper half of Fig. 3. As has been discussed earlier $\theta_1(x)$ shows a clear non-linearity between the limiting values $\theta_1(\text{GdAg}) = -106$ K and $\theta_1(\text{GdZn}) = +270$ K [14]. Unmixing phenomena, for instance, should give rise to sudden deviations from a smooth and continuous $\theta_1(x)$ behaviour in quite the same way as it has been considered for diamagnetically diluted systems [15]. Such a discontinuous $\theta_1(x)$ behaviour is not observed. In Ref. [14], the non-linear $\theta_1(x)$ behaviour has been explained by

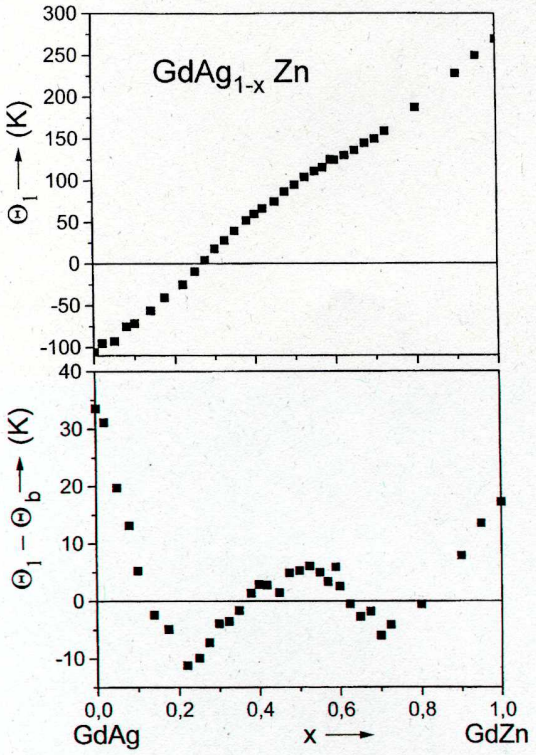

Fig. 3. Upper diagram: composition dependence of Curie–Weiss temperature θ_1 of the linear susceptibility χ_1. Lower diagram: fourth-order oscillatory part of θ_1 obtained after subtraction of a smooth background function $\theta_b(x)$.

attributing different exchange parameters to each of the five different possibilities to occupy the four intervening lattice sites between two nearest Gd^{3+} sites either by Zn or Ag atoms. This introduces terms with x^2, x^3 and x^4 to the $\theta_1(x)$ function. However, the appropriateness of this interpretation must be questioned in view of the observation made here that biquadratic interactions play a decisive role in the $GdAg_{1-x}Zn_x$ system. This additional interaction is known to affect the $\theta_1(x)$ values and the transition temperatures [16, 17] but to an unknown extent making a quantitative decomposition of the $\theta_1(x)$ data into contributions from both interaction types, a too complicated problem to be solved rigorously. In the lower part of Fig. 3 we show the oscillating portion of the $\theta_1(x)$ function obtained after subtraction of a smooth background function $\theta_b(x)$. This background function is a linear in the range $0.375 < x < 1.0$ with a small quadratic term added for $x < 0.375$. Since the background function $\theta_b(x)$ cannot be defined unambiguously, the result obtained for the oscillating part $\theta_1(x) - \theta_b(x)$ should be discussed only in a qualitative way.

In contrast to the interpretation tried in Ref. [4] we here propose to attribute the clearly visible fourth order x-dependence to biquadratic interactions. This interpretation makes sense in several respects:

First, it results that the biquadratic interaction of GdAg is ferromagnetic. This type of interaction is therefore in conflict with the antiferromagnetic order of GdAg and thereby explains the non-equilibrium magnetization phenomena observed below a well-defined temperature of $T_{ne} = 67$ K. As shown in Fig. 9 later, the temperature T_{ne} below which thermodynamic non-equilibrium phenomena occur exhibits a composition dependence which is very similar to that one of $\theta_1(x) - \theta_b(x)$ with a minimum at about $x = 0.25$.

Second, in the composition range of interest here $0.48 < x < 0.59$, the biquadratic interaction strength has a ferromagnetic maximum according to the results in the lower section of Fig. 3. This is a necessary prerequisite in order to attribute the novel ferrimagnetic phases observed in this composition range to the action of biquadratic interactions.

Third, the behaviour of $\theta_1(x) - \theta_b(x)$ is in accord with the observed destabilization of the antiferromagnetic and ferromagnetic phase at low temperatures in the range $0.35 < x < 0.46$ and $0.63 < x < 0.65$, respectively, since in both composition intervals the biquadratic interaction is opposite in sign to the leading bilinear interaction.

One further consequence of the just given interpretation is that the total biquadratic interaction is ferromagnetic for the pure systems GdAg and GdZn. This agrees with observations made for the europium monochalcogenides [1]. For these insulating materials a total ferromagnetic biquadratic interaction results by a strong ferromagnetic three-spin interaction and a weaker antiferromagnetic biquadratic interaction [12]. This conclusion has been drawn from the strong non-linear composition dependence of the biquadratic interaction strength in $Eu_xSr_{1-x}Te$ [3]. Also in the metallic

compound GdS the total biquadratic interaction is ferromagnetic [18].

3. Magnetic measurements

Starting from $x = 0$, the antiferromagnetic end of the system, and $x = 1$, the ferromagnetic one, it is straightforward to evaluate the variation of the Néel temperature $T_N(x)$ and the Curie temperature $T_C(x)$ with composition.

$T_N(x)$ shows a pronounced non-linear x-dependence (see Fig. 9) and even decreases somewhat for $x \to 0$. Since it is unlikely that this decrease is caused by a decreasing bilinear antiferromagnetic interaction or an increasing bilinear ferromagnetic interaction for $x \to 0$, we propose to explain the curved $T_N(x)$ behaviour by biquadratic interactions which apparently vary in a strongly non-linear way with composition as is qualitatively displayed in the lower panel of Fig. 3. We should note that also in the $Eu_xSr_{1-x}Te$ system the biquadratic interaction strength varies in a non-linear way with composition [3, 12]. The decreasing $T_N(x)$ line for $x \to 0$ is then explained by a strongly increasing ferromagnetic biquadratic interaction for $x \to 0$. This view is supported by the observation of non-equilibrium phenomena in susceptibility measurements performed in small fields ($B_0 < 0.5$ T). These could well be caused by the competition of antiferromagnetic bilinear interactions and ferromagnetic biquadratic interactions. Fig. 4 shows a field-cooled susceptibility measurement and a second measurement conducted for increasing temperature after cooling the sample without field. Both curves coincide for temperatures $T > T_{ne} = 67$ K in the case of GdAg. From this we may conclude that the strength of the ferromagnetic biquadratic interaction is about 67 K but the total biquadratic interaction may be smaller due to the additional presence of antiferromagnetic biquadratic interactions. As can be seen further from Fig. 9 the composition dependence of the non-equilibrium temperature $T_{ne}(x)$ conforms qualitatively well with that one of $\theta_1(x) - \theta_b(x)$ given in the lower half of Fig. 3, which we believe reflects reasonably well the composition dependence of the total biquadratic interaction strength.

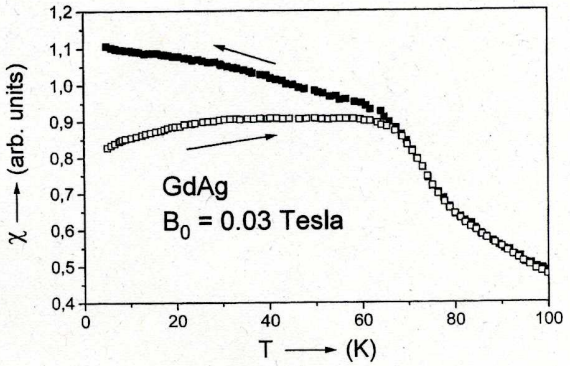

Fig. 4. Thermodynamic non-equilibrium phenomena as observed in susceptibility measurements on GdAg for fields $B_0 < 0.5$ T. Upper curve: field-cooled measurement, lower curve: zero-field-cooled measurement.

The curvature of the Curie line $T_C(x)$ is less pronounced, but $T_C(x)$ increases clearly with an increasing rate for $x \to 1$ [21, 22], which we interpret again by an increasing ferromagnetic biquadratic interaction for $x \to 1$.

Before both phase lines end new low-temperature anomalies appear in the ferromagnetic as well as in the antiferromagnetic phase. Typical $M(T)$ curves as they are characteristic for the different x-sections of the phase diagram are compiled in Fig. 5.

On the ferromagnetic side the new phenomenon arising close to the end of the $T_C(x)$ phase line consists in the fact that the demagnetization plateau observed for the spherical samples is no longer constant until the lowest temperature but shows a definite decrease in measurements with decreasing temperature (see upper left panel of Fig. 5). This conforms to an increase of the antiferromagnetic $\frac{1}{2}\frac{1}{2}0$ scattering intensity in the neutron diffraction spectra, as will be shown later on (see Fig. 15).

On the antiferromagnetic side a pronounced kink develops below the Néel temperature which shows up as an only weak kink not to be discernible in the representation given in the lower left panel of Fig. 5. It appears, therefore, that the ferromagnetic and the antiferromagnetic phase do not persist to the lowest temperatures near the limiting concentrations for their existence at $x = 0.63$ and 0.46,

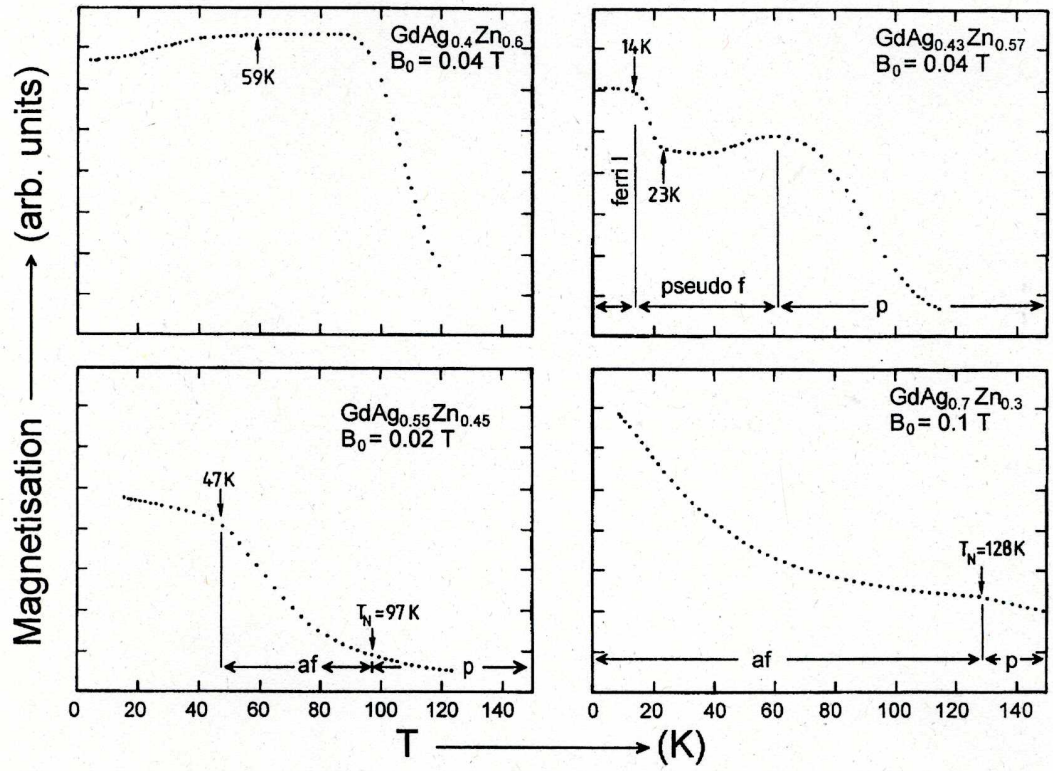

Fig. 5. Typical susceptibility curves as characteristics of the different parts of the $GdAg_{1-x}Zn_x$ system. Upper left panel: non-constant demagnetization plateau observed for samples near the end of the ferromagnetic range. Upper right panel: two fold plateau structure with a first-order transition into a state with a spontaneous magnetic moment (ferri I phase) at ≈ 23 K observed for samples with $0.48 < x < 0.59$. Lower left panel: in the composition range $0.35 < x < 0.46$ the recurrent Néel line $T_N(x)$ is crossed two times, at T_N (not to be resolved in this representation) and at a lower temperature below which the magnetization shows a weaker temperature dependence. Lower right panel: in the composition range $0 < x < 0.36$ one single anomaly at $T_N(x)$ is observed.

respectively, but they show a recurrent behaviour with ending points for $T \to 0$ at $x = 0.65$ for the $T_C(x)$ line and $x = 0.35$ for the $T_N(x)$ line. We mention these features which are very similar to those reported in Ref. [19] only for the sake of completeness without discussing them further.

The strongest of the novel magnetization anomalies with which we will be concerned here is seen in the upper right section of Fig. 5. In small fields the $M(T)$ curves show on the high-temperature side first a rounded shoulder with a nearly constant magnetization plateau towards lower temperatures. This first plateau value, however, does not conform to the demagnetization-limited value and therefore pertains to a finite susceptibility. At ≈ 23 K the magnetization rises again in a step-like way and the consecutive second plateau corresponds now to an infinite susceptibility. This composition-independent behaviour for the range $0.48 < x < 0.59$ is shown in more detail in Fig. 6 for another spherical sample with composition $x = 0.525$. In the intermediate part of the $GdAg_{1-x}Zn_x$ phase diagram under consideration, strong non-equilibrium magnetization phenomena are again noticeable as is demonstrated in Fig. 6. The field-cooled curve reaches a final magnetization value of $J/B_0 = 3$ in the limit $T \to 0$, indicative of a state with a spontaneous magnetic moment, but the zero-field-cooled

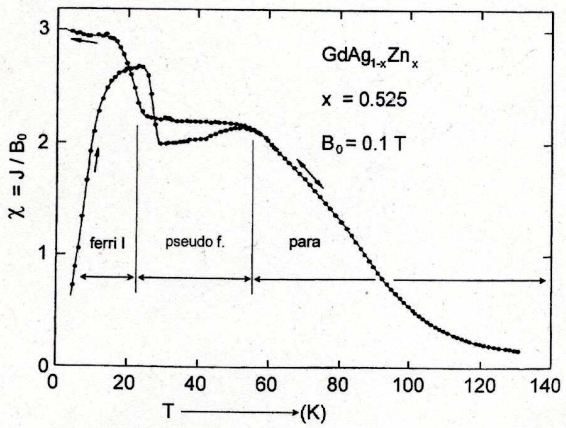

Fig. 6. Field-cooled and zero-field-cooled susceptibility curves for a sample with $x = 0.525$ showing pronounced hysteresis at the pseudoferromagnetic to ferri I transition. Nonequilibrium phenomena set in at the paramagnetic to pseudoferromagnetic phase transition.

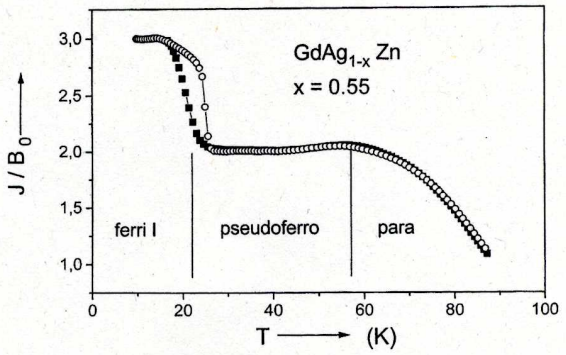

Fig. 7. Susceptibility measurements run down and up in temperature without switching of the field. Under this condition the hysteresis at the pseudoferromagnetic to ferri I transition is the only difference between both ways to proceed.

curve which is conducted for increasing temperatures starts with a considerably reduced magnetization value. In both curves the first order phase transition into the ferri I phase is clearly visible as a discontinuity showing the typical hysteresis. The field-cooled and zero-field-cooled curves coincide for temperatures larger than ≈ 55 K and this event marks a further phase transition, as will be confirmed with magnetostriction measurements later on. We call this phase extending between 25 and 55 K for which the susceptibility is always finite pseudoferromagnetic. If a field-cooled measurement is followed by a measurement for increasing temperatures without switching off the magnetic field, the hysteresis at the first-order transition remains as the only difference between the two ways to proceed (Fig. 7).

In view of the fact that no anomaly at all is observed in the neutron scattering spectra at $T \approx 25$ K, it appeared very important to confirm with specific heat measurements that the $T = 25$ K anomaly constitutes a true first-order magnetic phase transition. Therefore, the specific heat capacity of one sample with composition $GdAg_{0.45}Zn_{0.55}$ has been measured using an improved version of a vacuum calorimeter as described in Ref. [20]. The quasi-adiabatic step-heating method (Nernst method) was used. From the $c_p(T)$ data the contributions of the sapphire sample holder and the minute amount of grease by which the sample has been attached were subtracted. In Fig. 8 we have plotted $\Delta c_p(T)$ obtained from $c_p(T)$ after subtraction of a smooth background function fitted to both sides of the observed phase transition. The small but sharp peak at 25.5 ± 0.3 K which is about 2.5% of the total signal, confirms in fact the existence of a first-order phase transition. The transition enthalpy (latent heat) of ≈ 0.5 J/mol is, however, orders of magnitude smaller than that one of common structural phase transitions (some kJ/mol). Applying small fields (0.25 T) the peak broadens rapidly and shifts to higher temperatures as is observed with magnetization and magnetostriction measurements (see Figs. 11 and 19). The enthalpy increases rapidly with field but the character of the phase transition is no longer clear. It may be some mixture between first and second order.

The susceptibility anomalies as they are exemplified by the four diagrams of Fig. 5 have been combined with the neutron scattering and magnetostriction results, to be discussed below, to construct the $GdAg_{1-x}Zn_x$ phase diagram for zero external field. As can be seen from Fig. 9, this phase diagram reveals some symmetry and resembles the one given in Ref. [19] for $Dy_{1-x}Y_xMn_2$. The prominent feature of the $GdAg_{1-x}Zn_x$ phase diagram is the existence of an intermediate buffer zone

the non-equilibrium temperatures T_{ne} as far as these have been investigated in detail. In the range $0.48 < x < 0.59$ $T_{ne}(x)$ seems to coincide with the pseudoferromagnetic to paramagnetic phase boundary.

If two consecutive phase transitions as a function of temperature are observed in susceptibility measurements, as in Figs. 6 and 7, it is also likely that measurements as a function of field will reveal phase transitions. This is correct, as demonstrated in Fig. 10. Here, two magnetic isotherms are seen for $T = 4$ and 40 K. To obtain the equilibrium magnetization values each data point has been taken after cooling the sample in the specified field from a sufficiently high temperature ($T > 60$ K) where thermal equilibrium applies. Fig. 10 also includes the calculated demagnetization line $J = 3B_0$ for both magnetization curves as it results from the theoretical magnetic induction (magnetic density) using a demagnetization factor of $\frac{1}{3}$ for the spherical samples used here. This line marks a vanishing internal field according to $B_i = B_0 - \frac{1}{3}J$, viz. an infinite magnetic susceptibility. For the $T = 4$ K curve (upper-field scale) the reduced magnetization data with $m \leqslant \frac{1}{3}$ fall on this demagnetization line, thus indicating a state with a ferrimagnetic order with a spontaneous saturation magnetization of $m_s \cong \frac{1}{3}$. This is in contrast to the $T = 40$ K curve (lower-field scale) which starts also with a linear field dependence but the associated slope is smaller than the demagnetization line. The change from a linear to a curved magnetization behaviour at about 0.3 T as seen for the $T = 40$ K indicates a magnetic phase transition as is evidenced with magnetostriction measurements. This anomaly (pseudoferromagnetic to paramagnetic phase transition) marks the field limit of the pseudoferromagnetic phase. This phase is characterized by a linear relation between magnetization and field and by the occurrence of temperature-independent plateau values in magnetization measurements as a function of temperature like those seen in Fig. 7. Both features resemble those of a ferromagnet with the only difference that here the susceptibility is always finite. For fields larger than 0.3 T, viz. in the paramagnet state, the magnetization $M(T)$ changes to a monotonously increasing behaviour with decreasing temperature. Also the obtuse kink which can be noticed in the $T = 4$ K magnetization curve at about 1.1 T marks a field-induced phase transition (ferri I to ferri II phase) as again confirmed with magnetostriction measurements. It is particularly interesting to note that both magnetization events in the $T = 4$ K curve are rather weak and occur near magnetization values of $\frac{1}{3}$ and $\frac{2}{3}$.

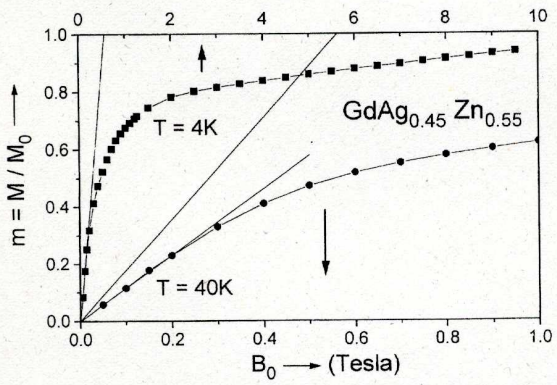

Fig. 10. Magnetization curves at $T = 4$ K (upper field scale) and $T = 40$ K (lower field scale) for one sample of the range $0.48 < x < 0.59$ with $x = 0.55$. While the $T = 4$ K curve starts with the calculated demagnetization line (solid straight line), the initial slope of the $T = 40$ K curve is distinctly below the demagnetization line as is indicative for a state with a finite susceptibility.

The just outlined magnetization anomalies have been combined with the magnetostriction results to construct the magnetic phase diagram as it is common to all samples with $0.48 < x < 0.59$ (Fig. 11). This phase diagram includes two ferrimagnetic phases labelled ferri I and ferri II with ground-state saturation magnetization values of $m = \frac{1}{3}$ and $m = \frac{2}{3}$, respectively. Additionally, the just mentioned pseudoferromagnetic phase follows for higher temperatures, which looks ferromagnetic but since the susceptibility is always finite there is no true spontaneous magnetic moment. This phase exists only for small internal fields of the order of 0.1 T. An external field penetrates from the beginning into the sample in the pseudoferromagnetic phase without being shielded completely by magnetic domains (demagnetization effects). For larger fields the pseudoferromagnetic phase transforms into the paramagnetic phase and this occurs at a magnetization value of $m \approx 0.25$.

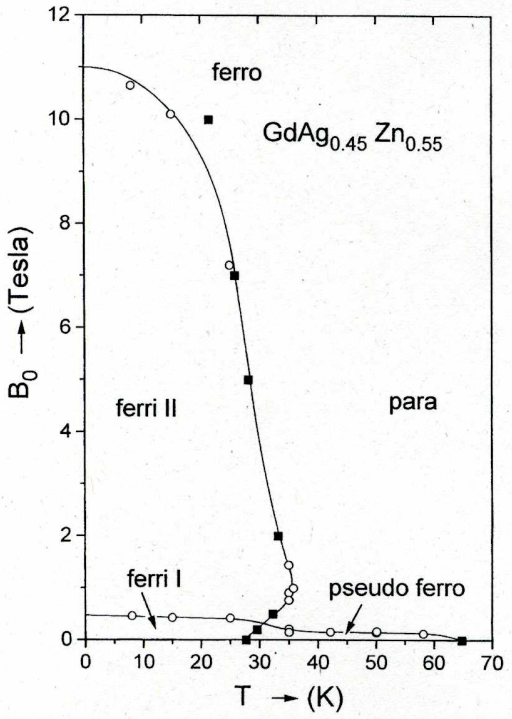

Fig. 11. The typical magnetic phase diagram for the samples of the composition range $0.48 < x < 0.59$ as set-up with dilatometric and magnetization measurements. Filled symbols mark those anomalies observed in measurements as function of temperature, while open symbols give anomalies observed in measurements as function of field.

According to the magnetization, dilatometric and specific heat measurements, the phase boundary between the ferri I phase and the pseudoferromagnetic phase is evidently first order. All other phase lines seem to be second order, but care is required since magnetization measurements allow no definite decision as regards the order of the phase transition. In Ref. [3], for instance, it has been observed with neutron scattering that phase transitions which are caused by biquadratic interactions are first order in $Eu_xSr_{1-x}Te$ although the magnetization behaves continuous at these phase boundaries. The proposed magnetic phase diagram exhibits one vertex point at which all ordered phases seem to coexist. Little is known about the allowed types of magnetic vertices, in particular if the phase boundaries are caused by biquadratic interactions [23].

The magnetic phases occurring in the phase diagram in Fig. 11 and their properties are very unusual. In particular, the pseudoferromagnetic phase which is stable in finite magnetic fields cannot be explained with bilinear exchange interactions alone. It is very important to note that the phase transition between the paramagnetic and the pseudoferromagnetic phase occurs at a finite susceptibility and that the susceptibility remains finite over the whole temperature range where the pseudoferromagnetic phase exists. A finite susceptibility at T_c has been found to be a characteristic signature of biquadratic-exchange interactions [24–26]. Moreover, it appears likely that the different ordered phases in the magnetic phase diagram of Fig. 11 are determined completely by biquadratic-exchange interactions.

The simplest way to identify those interactions is a molecular field analysis of the high-temperature paramagnetic data. This method has been described in Ref. [1]. In the high-temperature approximation the relation between the applied magnetic field B_0 (which has to be converted to its value inside the sample B_i) and the reduced magnetization m can be written as

$$B_i = \frac{1}{\chi_1} m + \frac{1}{\chi_3} m^3 + \cdots \tag{1}$$

This equation is the derivative of the Landau free-energy potential with respect to the order parameter m. As is well known, the linear susceptibility χ_1 obeys a Curie–Weiss law in the high-temperature approximation which reads according to the nomenclature used in Ref. [1]:

$$\chi_1 = \frac{C_1}{T - \theta_1} \quad \text{with } C_1 = \frac{g(S+1)\mu_B}{3k_B}. \tag{2}$$

The following discussion is restricted to a system with pure spin magnetism for which crystal-field contributions to the Curie–Weiss temperature θ_1 can be neglected. θ_1 is like the ordering temperature not only given by bilinear exchange interactions but to some extend also by four-spin interactions [16, 17]. Interestingly, the cubic susceptibility also obeys a Curie–Weiss law given by

$$\chi_3 = \frac{C_3}{T - \theta_3} \quad \text{with } C_3 = \frac{10g(S+1)^3\mu_B}{9[(S+1)^2 + S^2]k_B}. \tag{3}$$

In contrast to θ_1, θ_3 is a measure for four spin, three spin and biquadratic interactions alone [3]. These interactions are all fourth-order perturbation processes. To evaluate χ_3, high-temperature paramagnetic isotherms are measured and plotted as m^2 versus B_i/m (Arrott plot). These measurements have to be conducted to sufficiently high field values until a clear curvature becomes visible in the magnetic isotherms. Fig. 12 displays some magnetization curves for a $GdAg_{0.45}Zn_{0.55}$ sample plotted as m^2 vs. B_i/m. According to (1) the slopes of the Arrott isotherms give the cubic susceptibility χ_3 and the intersections with the abscissa the reciprocal linear susceptibility χ_1^{-1}. As can be seen in Fig. 12, the Arrott isotherms are linear over a considerable magnetization, viz. field range. This applies, however, only for stoichiometric material. For non-stoichiometric material the Arrott isotherms are not linear at all, as has also been observed for the insulating europium monochalcogenides [1]. The linearity of the Arrott isotherms is therefore a very sensitive means to control the homogeneity and/or stoichiometry of the samples.

To verify the anticipated Curie–Weiss law of the cubic susceptibility, χ_3^{-1} is plotted versus temperature as it is common for the linear susceptibility. In contrast to the insulating europium monochalcogenides χ_3 does, however, not approach the Curie–Weiss law even at more than five times the ordering temperature in the present metallic $GdAg_{1-x}Zn_x$ system (Fig. 13). This has also been observed in GdS which is also a metallic system with strong biquadratic interactions [18]. The behaviour of χ_3 is at variance with that one of χ_1 which reaches the Curie–Weiss regime satisfactorily already at temperatures larger than two times the ordering temperature. Fig. 13 includes the Curie line $\chi_3^{-1} = C_3^{-1} \cdot T$ as it can be calculated with the expression for the cubic Curie constant C_3 according to (3) inserting $g = 2$ and $S = \frac{7}{2}$. The behaviour of χ_3^{-1} is not only uncommon on account of a missing Curie–Weiss behaviour but also by the fact that χ_3 varies between larger and smaller values referred to the Curie law, as it characterizes the case without biquadratic interactions ($\theta_3 = 0$). This could mean that the different biquadratic interaction processes of both signs are much stronger

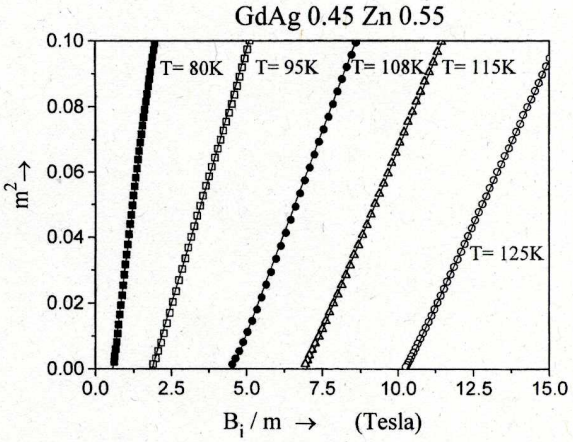

Fig. 12. Paramagnetic isotherms for one sample with $x = 0.55$ plotted as m^2 vs. B_i/m (Arrott plot). The slopes of these lines give the cubic susceptibility χ_3 and the intersections with the abscissa the reciprocal linear susceptibility χ_1^{-1}.

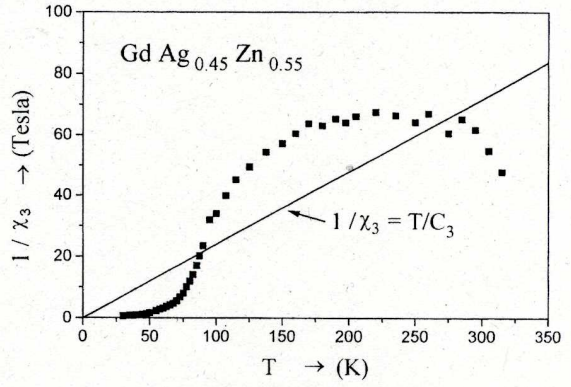

Fig. 13. Reciprocal cubic susceptibility χ_3^{-1} vs. temperature for $GdAg_{0.45}Zn_{0.55}$. The solid line gives the calculated Curie law for χ_3. Deviations below $1/\chi_3$ mean ferromagnetic biquadratic correlations, while deviations above $1/\chi_3$ mean antiferromagnetic biquadratic correlations.

than the observed macroscopic average and have all a different and strong temperature dependence such that the observed temperature dependence of χ_3 results by a superposition of all these processes. It is particularly surprising that the alternations between ferromagnetic and antiferromagnetic correlations take place more rapidly with temperature than

known for the linear susceptibility which remains either entirely larger or smaller than the Curie law with $\theta_1 = 0$.

Our aim to obtain a quantitative measure for the strength of biquadratic interactions by the evaluation of θ_3 thus failed, since χ_3 does not show a Curie–Weiss behaviour in the accessible temperature range. The only conclusion we can draw from the fact that χ_3 deviates strongly from the calculated Curie law is that the resulting biquadratic interaction is ferromagnetic for $T < 85$ K and antiferromagnetic for $T > 85$ K with averaged interaction energies reaching ≈ 30 K and ≈ 80 K, respectively. It is intuitively clear that a very strong competition between ferromagnetic and antiferromagnetic biquadratic interactions as inferred from the non-Curie–Weiss behaviour of χ_3 and its alternations between ferromagnetic and antiferromagnetic correlations will result in a strongly non-collinear magnetic order which is hard to detect with scattering methods. A total ferromagnetic biquadratic interaction value of the order of 30 K for $T < 85$ K supports the view that the magnetic phases in the phase diagram of Fig. 9 are the results of biquadratic interactions under which the ferromagnetic ones dominate. As a rule of thumb, the ordering temperature for zero field, T_{crit}, and the critical field for $T \to 0$, $B_c(T \to 0)$, should be related by the cubic Curie constant C_3 according to

$$T_{crit} = C_3 \cdot B_c(T \to 0) \tag{4}$$

if the magnetic order is mainly due to biquadratic interactions. In the case of dominating bilinear interactions C_3 has to be replaced by C_1. Using $C_3 = 4.186\ \mathrm{K}/T$ for a spin system with $S = \frac{7}{2}$ one calculates with $B_c(T \to 0) = 11$ T an ordering temperature of 46 K, which is at least much closer to the observed one of $T_{crit.} \cong 57$ K compared to the alternative calculation with $C_1 = 2.015\ \mathrm{K}/T$.

As a consequence, there are many pieces of evidence that the novel magnetically ordered states observed in the intermediate composition range of the $GdAg_{1-x}Zn_x$ system are caused by biquadratic interactions and the neutron-diffraction studies to follow support this view although indirectly and with unexpected results.

4. Neutron diffraction experiments

Due to the strongly increasing neutron absorption cross-section of Gd with increasing neutron wavelength, diffraction experiments have been carried out partly on instrument D5 installed at the hot neutron source of the high-flux reactor of the Institute Laue-Langevin in Grenoble, France using a wavelength of 0.044 nm, but mostly on instrument D4 using a wavelength of 0.050 nm. For these experiments the $GdAg_{1-x}Zn_x$ ingots have been machined into granular turnings, which were filled into an 1 mm thick annular space between two concentric vanadium cylinders fabricated from thin vanadium sheets. For the antiferromagnetic material GdAg the results of a single-crystal study [27] and a powder diffraction experiment [14] have been reported elsewhere and will therefore be discussed only in short here. Fig. 14 compiles four magnetic diffraction spectra of the $GdAg_{1-x}Zn_x$ system, which show the gradual intensity change from the antiferromagnetic to the ferromagnetic Bragg positions.

According to the observed selection rules for the magnetic scattering intensities of GdAg (odd–odd–even half-integers) the magnetic unit cell is doubled only along two space directions. Equal moments are found on (1 1 0) planes with moment orientations along that space direction for which the magnetic unit cell is not doubled. This information can be inferred from an investigation of the relative intensities of the half-integer odd–odd–even indexed magnetic superstructure reflections since the magnetic unit cell has a tetragonal symmetry and therefore one preferred axis [28]. It should be noted that the evaluated spin structure of GdAg conforms to that one reported earlier for TbCu [29].

Typical neutron diffraction spectra as they are characteristic for the situation near the end of the ferromagnetic phase are shown in Fig. 15. In the upper half the magnetic intensities at $T = 60$ K are seen which are obtained by subtracting from the $T = 60$ K spectrum a spectrum measured at $T = 117$ K which is at a temperature where the magnetic intensities are much suppressed. Even though pronounced magnetic scattering lines appear in this spectrum a line width analysis shows

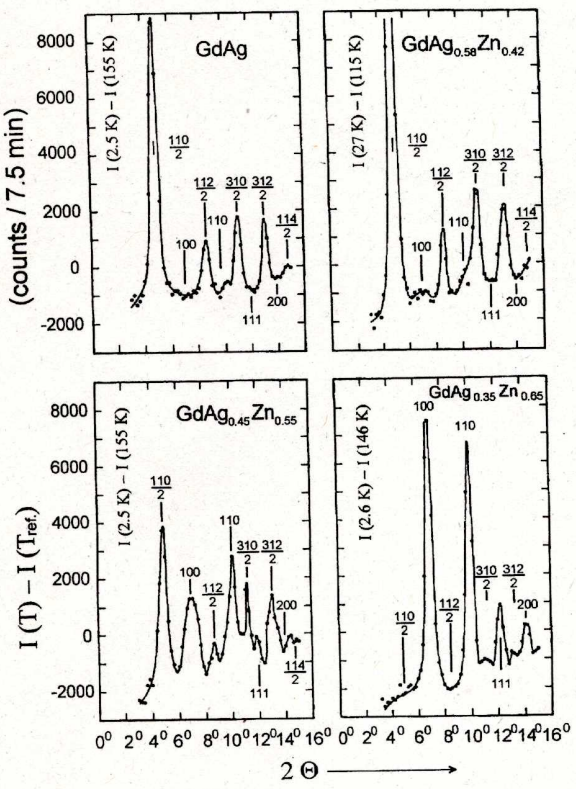

Fig. 14. Selected magnetic neutron scattering spectra showing the gradual intensity change from the antiferromagnetic odd–odd–even half-integer intensities to the ferromagnetic ones. At intermediate compositions the magnetic scattering intensities are due to short-range order as revealed by the increased line width.

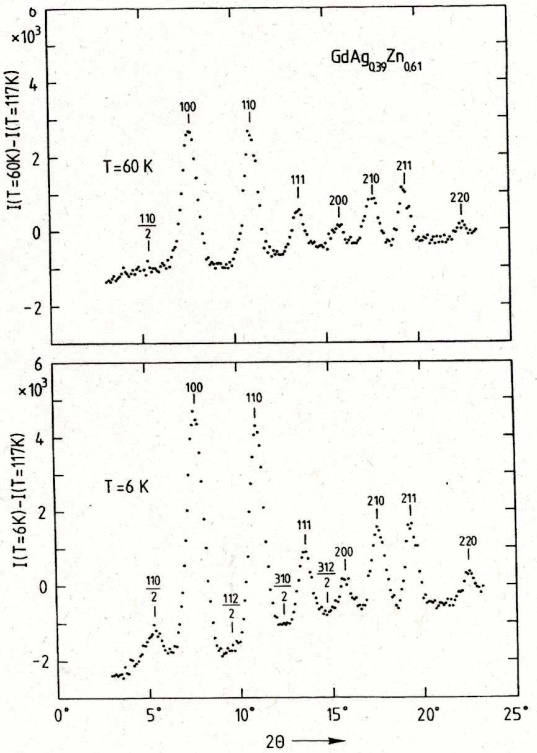

Fig. 15. Magnetic neutron scattering spectra for one $GdAg_{1-x}Zn_x$ sample with $x = 0.61$. Rather intense but broadened lines are observed. At low temperatures an antiferromagnetic $\frac{1}{2}\frac{1}{2}0$ intensity appears additionally, indicating destabilization of the ferromagnetic correlations.

that the magnetic scattering lines are broader than the nuclear scattering lines observed near the same 2θ positions at a sufficiently high temperature. This shows that there is no long-range ferromagnetic order at $x = 0.61$. A similar ambiguity arises also in the magnetization measurements since these resemble also very much those of a long-range ordered system. Here, only a careful linewidth analysis of the neutron scattering lines can help in deciding whether a long-range magnetic order is given or not. The accuracy of this method is however badly limited using a neutron wavelength of only 0.044 nm like in the present experiment. For the nuclear scattering lines a full line width at half-maximum of $\Delta 2\theta \approx 0.45^\circ$ is observed which corresponds to a resolution of the scattering vector of $\Delta Q \approx 63\ \mathrm{nm}^{-1}$. Therefore, if the magnetic scattering lines are broadened with respect to the nuclear ones this indicates a short-range order with a correlation length of only ≈ 0.02 nm, which is even much less than the spacing between the magnetic moments of 0.36 nm.

In the $T = 6$ K spectrum shown in the lower part of Fig. 15 a scattering intensity at the antiferromagnetic $(\frac{1}{2}\frac{1}{2}0)$ position is seen additionally, which indicates the tendency of the system to destabilize the ferromagnetic state at low temperatures. This observation conforms to the decreased demagnetization plateau in the magnetization measurements shown in the upper left panel of Fig. 5.

The result of a line width analysis for the ferromagnetic 100 intensity is shown in Fig. 16. These data show that there is definitely no long-range ferromagnetic order for $x < 0.61$. Even the fact that for the $x = 0.62$ sample the 100 line width drops in an intermediate temperature interval below the experimental resolution limit is only a necessary but not a sufficient criterion for a long-range ferromagnetic order. With some arbitrariness we therefore like to limit the ferromagnetic phase to $x > 0.63$. In any case, there is a composition gap of the order $3 \pm 1\%$ between the ferromagnetic phase and the new magnetic ordering structures found in the range $0.48 < x < 0.59$. This gap gets even larger for $T \to 0$ as can be concluded from the re-increasing line width of the 100 reflection of the $x = 0.62$ sample for $T < 30$ K in Fig. 16, indicating a destabilization of the ferromagnetic correlations for low temperatures.

Also on the antiferromagnetic side of the system the line-broadening phenomena indicate the limit of the antiferromagnetic phase as can be seen in Fig. 17 for the $\frac{1}{2}\frac{1}{2}0$ intensity. This diagram displays two-line profiles on a logarithmic scale. The parabola fitted through the experimental points verify the Gaussian character of the line profiles but for both lines the full-widths at half-maximum are larger than those observed for the nuclear reflections. These nuclear line widths are indicated by horizontal bars for comparison. Thus, only line width considerations and not line intensities as function of composition allow a decision on the limits of the antiferromagnetic and ferromagnetic phase.

The magnetic scattering intensities as are seen in the lower left diagram of Fig. 14 for a sample with $x = 0.55$ have nothing to do with the magnetization

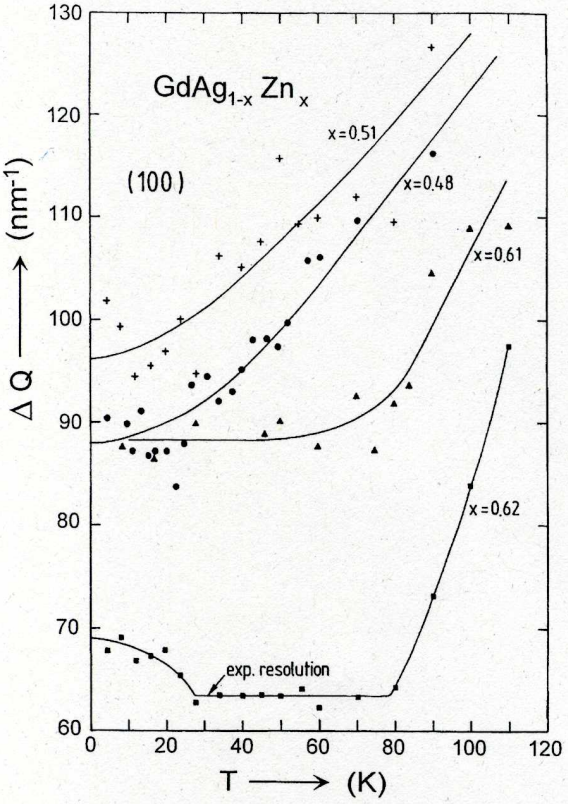

Fig. 16. Temperature dependence of the line width of the ferromagnetic 100 reflections. Although the magnetic line width of the $x = 0.62$ sample drops below the resolution limit of the D4 instrument in the intermediate temperature interval 30 K $< T <$ 80 K, there is not necessarily a true long-range magnetic order for this composition.

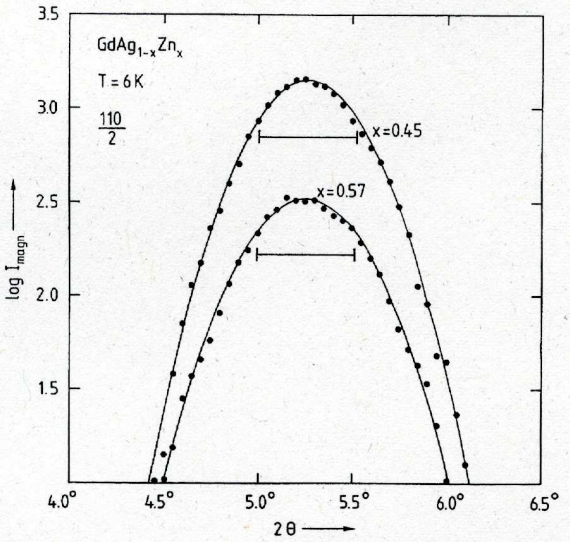

Fig. 17. Line profiles of the antiferromagnetic $\frac{1}{2}\frac{1}{2}0$ intensity for two samples with $x = 0.45$ and 0.57 given on a logarithmic scale. The parabola fitted through the experimental data demonstrate the Gaussian character of the lines but the observed full-widths at half-maximum are larger than the instrumental resolution evaluated by the width of the nuclear scattering lines (horizontal bars).

anomalies shown in the upper right panel of Fig. 5 or in Figs. 6 and 7. This becomes apparent by inspection of Fig. 18 which shows the temperature dependence of the integrated scattering intensities for the most intense ferromagnetic and antiferromagnetic line. For the samples of the composition range $0.48 < x < 0.59$ the ferromagnetic 100 scattering intensity shows no anomaly at all at about $T = 23$ K, where the susceptibility exhibits a sudden and strong increase with decreasing temperature. From this observation we have to conclude that the magnetic phase transitions at 58 K (paramagnetic to pseudoferromagnetic) and 23 K (pseudoferromagnetic to ferri I) are into states with strongly inhomogeneous or fluctuating spin structures and are therefore not accessible to an investigation with conventional scattering methods. This is not unlikely in view of the recent neutron scattering results on $Eu_xSr_{1-x}Te$ which showed that the antiferromagnetic MnO superstructure reflection intensities are substantially reduced and decrease further with diamagnetic dilution in this random site system [3]. Such a behaviour can easily be rationalized by the competition of antiferromagnetic bilinear and ferromagnetic biquadratic interactions in $Eu_xSr_{1-x}Te$. A diamagnetic dilution seems further to frustrate a homogeneous and collinear magnetic order.

The competition between antiferromagnetic and ferromagnetic biquadratic interactions is even more severe in the metallic $GdAg_{1-x}Zn_x$ system, since the individual interaction processes seem to be much stronger in metals as is evidenced by the non-Curie–Weiss behaviour of χ_3. As a result, the magnetic order induced by those competing biquadratic interactions may be strongly non-collinear.

The only indirect indication that an ordering process takes place at about 60 K in the $GdAg_{1-x}Zn_x$ samples with $0.48 < x < 0.59$ is given by the temperature dependence of the magnetic diffuse small-angle scattering intensities which stop increasing further with decreasing temperature at about 60 K.

In conclusion, it can be said that neutron scattering allows to delineate the phase regions possessing a conventional magnetic order, e.g. the antiferromagnetic and ferromagnetic phase but on the condition that the composition limits of these phases must be elaborated with line-broadening investigations. The new magnetic ordering structures of the range $0.48 < x < 0.59$ which can be assumed to be stabilized mainly by biquadratic interactions are apparently not accessible to standard neutron-scattering investigations.

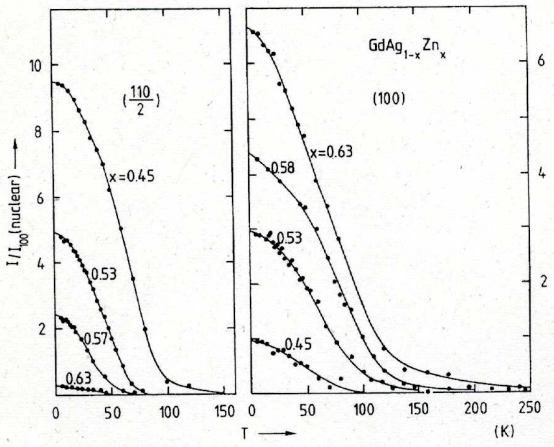

Fig. 18. Integrated magnetic scattering intensities for the antiferromagnetic $\frac{1}{2}\frac{1}{2}0$ and the ferromagnetic 2 0 0 reflection. Without considering the line widths these data allow no definite decision on the limits of the ferromagnetic antiferromagnetic phase.

5. Dilatometric measurements

The temperature and magnetic-field-induced length changes of one sample of the range $0.48 < x < 0.59$ with composition $GdAg_{0.45}Zn_{0.55}$ were measured with a capacitance dilatometer designed for measurements of the thermal expansion coefficient $\alpha = (1/L)\partial L(T)/\partial T$ in magnetic fields. The main difference between this dilatometer and our conventional one [30] is a thermal decoupling between the sample and the plate capacitor. Thus, the cell effect arising from the thermal expansion of the dilatometer is distinctively reduced. The thermal expansion coefficient is derived from the detected length changes while the temperature is continuously increased (or decreased) with a constant rate of 2–3 mK/s. Besides the measurements of α in magnetic fields, the dilatometer also allows

for measurements of the magnetostriction, i.e. the field-induced length changes $\Delta L(B)/L(0)$ at constant temperatures. The magnetostriction is measured during a magnetic field sweep form 0 to 14 and back to 0 T with a rate of 4 mT/s. The dilatometer was calibrated by measuring the thermal expansion of aluminium and the magnetostriction of silicon. For a 5 mm sample the absolute accuracy is better than 10^{-6}/K and 5×10^{-7} for the thermal expansion and magnetostriction, respectively. The relative resolution (scatter of the data) for both quantities is at least one order of magnitude higher.

Fig. 19 shows the thermal expansion coefficient of $GdAg_{0.45}Zn_{0.55}$ in magnetic fields between 0 and 10 T as given in the figure. The inset gives an expanded view of the additional anomaly occurring at $\cong 65$ K in zero-magnetic field which we identify with the paramagnetic to pseudoferromagnetic phase transition. The data are recorded with increasing temperature. Measurements with decreasing temperature yield similar anomalies, but pronounced hysteresis effects are found for the transitions around 25 K in fields up to 1 T.

Fig. 20 compiles some magnetostriction measurements of $GdAg_{0.45}Zn_{0.55}$ at different temperatures given in the figure. The insets in the upper panels (50 and 70 K) give an expanded view of the field range up to 1 T. The insets in the lower panels show the field derivatives $(1/L)\partial L/\partial B$ to visualize the additional phase transitions at $B \geqslant 8$ T better. As we have mentioned earlier, the observed anomalies in the magnetostriction and thermal expansion are mostly resolved much better than the

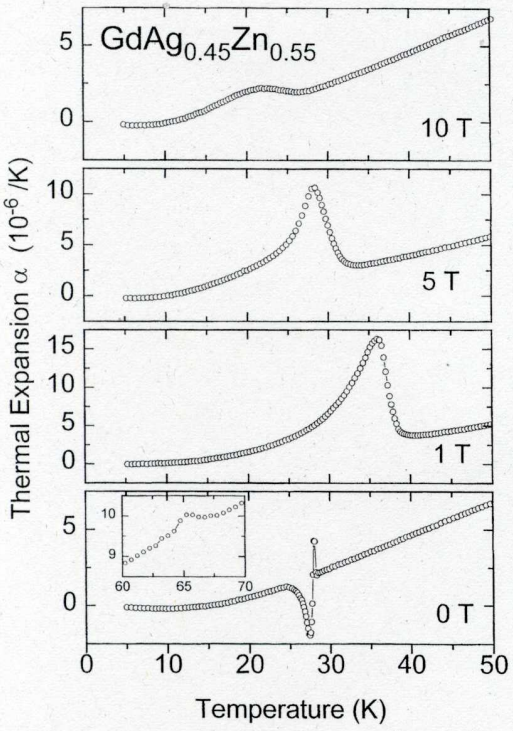

Fig. 19. Thermal expansion measurements in different magnetic fields. Inset in the $B_0 = 0$ T measurement shows a small anomaly near 65 K to be identified with the paramagnetic to pseudoferromagnetic phase transition.

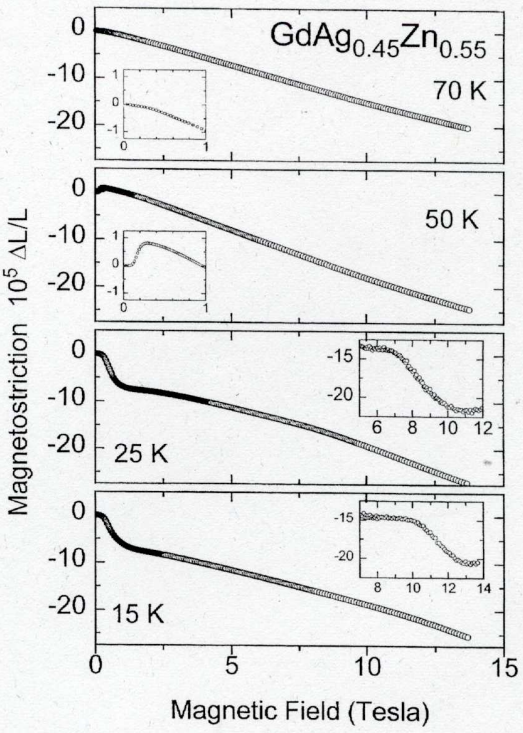

Fig. 20. Magnetostriction measurements for different temperatures. The inset in the $T = 70$ and 50 K curves give the initial behaviour on an expanded scale. Insets in the $T = 25$ and 15 K diagrams show the first derivatives for a better visualization of the high-field anomalies.

corresponding anomalies in magnetization and susceptibility measurements and allow a reliable set-up of the magnetic phase diagram as given in Fig. 11. In particular, the high-field thermal expansion measurements are clearly superior to susceptibility measurements if magnetic phase transitions are to be detected.

6. Conclusions

Biquadratic interactions can be investigated conveniently in systems with relatively weak bilinear interactions. In the $GdAg_{1-x}Zn_x$ system investigated here, the effect of bilinear interactions is greatly diminished by a compensation of the ferromagnetic interactions of GdZn with the antiferromagnetic ones of GdAg. Fortunately, biquadratic interactions are not suppressed in a similar way; on the contrary, they have a relative maximum near $x = 0.5$. The new magnetic ordering structures observed for $0.48 < x < 0.59$ can therefore be assumed to be stabilized by biquadratic interactions. Dilatometric measurements turned out to be the most efficient method in elaborating the boundaries of these new magnetic phases while neutron scattering failed in detecting any long-range magnetic order. This also shows that the magnetic order in these new phases differs much from those in the antiferromagnetic and ferromagnetic phases. Since the observed neutron scattering lines are considerably broadened near $x = 0.5$, these intensities can be assigned to spatially very small regions. As found earlier in $Eu_xSr_{1-x}Te$ [1, 3] phase boundaries due to biquadratic interactions do not come in contact with phase boundaries due to bilinear interactions. According to this observation it seems appropriate to distinguish between two-spin kind and four-spin kind transitions.

The new magnetically ordered phases observed in the composition range $0.48 < x < 0.59$ have very unusual properties. In particular, the pseudoferromagnetic phase which extends between 25 and 59 K has nearly ferromagnetic properties but the susceptibility always remains finite within this phase. For internal fields larger than only 0.1 T this pseudoferromagnetic phase transforms into the paramagnetic phase. Two further uncommon phases were identified labelled ferri I and ferri II. The ferri I phase is stable at low temperatures and has a spontaneous magnetic moment of very nearly $\frac{1}{3}$. This phase transforms into the ferri II phase at internal fields of about 0.6 T. At this phase boundary the magnetization has assumed a value of nearly $\frac{2}{3}$. A ferrimagnetic state with a spontaneous magnetic moment of $\frac{1}{3}$ is particularly difficult to imagine on a simple cubic lattice. Such ordering structures are evidently stabilized by the additional presence of antiferromagnetic biquadratic interactions which require a perpendicular moment orientation. Those interactions can be assumed to be always present regardless of the sign of the total biquadratic interaction. No complete ferromagnetic saturation seems to be reached even in the high-field ferri II phase.

Surprisingly, the cubic susceptibility does not approach the anticipated Curie–Weiss law even at five times the ordering temperature. A quantitative evaluation of the strength of the biquadratic interactions was thus not possible. From the missing Curie–Weiss law of χ_3 we have to conclude that the individual interaction processes which are all to be included in the class of four-spin interactions are very large and have different signs and different temperature dependencies such that the observed $\chi_3(T)$ behaviour can be considered the result of a superposition of all ferromagnetic and antiferromagnetic biquadratic interactions. The rapid alternations of χ_3 between ferromagnetic ($T < 85$ K) and antiferromagnetic ($T > 85$ K) four-spin correlations as function of temperature would then be given by a different temperature dependence of ferromagnetic and antiferromagnetic biquadratic interactions which are simultaneously present. The strongly non-collinear magnetic order in the new magnetic phases which are stabilized by biquadratic interactions is then the natural consequence of the severe competition between ferromagnetic and antiferromagnetic biquadratic interactions. This competition leads to ordering temperatures which can be assumed to be small compared with the strength of the individual interaction processes and leads to magnetic structures with virtually no translational symmetry such that conventional scattering methods become useless. A similar argument may be used to explain the strange composition

dependence of the total biquadratic interaction strength reflected by the fourth-order non-linearity of the $\theta_1(x)$ function which is visualized in the lower diagram of Fig. 3. This fourth-order function may also result by a superposition of the different composition dependencies of the different biquadratic interaction processes, as has been found for the $Eu_xSr_{1-x}Te$ system in Refs. [1, 3, 12].

Acknowledgements

We thank C. Freiburg for performing the lattice parameter evaluations of our samples. The technical assistance of B. Olefs is gratefully acknowledged.

References

[1] U. Köbler, R. Mueller, L. Smardz, D. Maier, K. Fischer, B. Olefs and W. Zinn, Z. Phys. B 100 (1996) 497.
[2] W. Zinn, J. Magn. Magn. Mater. 3 (1976) 23.
[3] R. Mueller, U. Köbler, K. Fischer, H.-A. Graf, A. Hoser, M.-T. Fernandez-Diaz, Z. Physik, to appear.
[4] U. Köbler, W. Kinzel and W. Zinn, J. Magn. Magn. Mater. 25 (1981) 124.
[5] J. Adler and J. Oitmaa, J. Phys. C 12 (1979) 575.
[6] V.M. Matveev and E.L. Nagaev, Sov. Phys. Solid State 14 (1972) 408.
[7] T. Iwashita and N. Uryu, J. Phys. C 21 (1988) 4783.
[8] R. Griessen, M. Landolt and H.R. Ott, Solid State Commun. 9 (1971) 2219.
[9] G. Petrich and T. Kasuya, Solid State Commun. 8 (1970) 1625.
[10] P. Fischer, W. Hälg, W.v. Wartburg, P. Schwob and O. Vogt, Phys. Kond. Mat. 9 (1969) 249.
[11] T. Sakakibara and M. Date, J. Phys. Soc. Japan 53 (1984) 3599.
[12] U. Köbler, I. Apfelstedt, K. Fischer, W. Zinn, E. Scheer, J. Wosnitza, H.v. Löhneysen and Th. Brückel, Z. Phys. B 92 (1993) 475.
[13] K.H.J. Buschow, Rep. Prog. Phys. 42 (1979) 1373.
[14] U. Köbler, J. Schweizer, P. Chieux and W. Zinn, J. Physique Colloque C8 49 (1988) 1099.
[15] K. Binder, Solid State Commun. 42 (1982) 377.
[16] R.G. Munro and M.D. Girardeau, J. Magn. Magn. Mater. 2 (1976) 319.
[17] F.C. SaBarreto and O.F. de Alcantara Bonfim, Physica A 172 (1990) 378.
[18] Th. Brückel, D. Drewes, K. Mattenberger, U. Köbler, W. Schnelle and G. Chouteau, to be published.
[19] C. Ritter, R. Cywinski, S.H. Kilcoyne, S. Mondal and B.D. Rainford, Phys. Rev. B 50 (1994) 9894.
[20] E. Gmelin, Thermochimica Acta 110 (1987) 183.
[21] J. Rouchy, P. Morin and E. du Tremolet de Lacheisserie, J. Magn. Magn. Mater. 23 (1981) 59.
[22] K. Eckrich, E. Dormann, A. Oppelt and K.H.J. Buschow, Int. J. Magn. 5 (1973) 75.
[23] S.K. Yip, T. Li and P. Kumar, Phys. Rev. B 43 (1991) 2742.
[24] R. Aleonard, P. Morin, J. Pierre and D. Schmitt, Solid State Commun. 17 (1975) 599.
[25] K.H.J. Buschow and C.J. Schinkel, Solid State Commun. 18 (1976) 609.
[26] U. Köbler, R. Mueller and J. Brown, to be published.
[27] T. Chattopadhyay, G.J. McIntyre and U. Köbler, Solid State Commun. 100 (1996) 117.
[28] G. Shirane, Acta Crystallogr. 12 (1959) 282.
[29] J.W. Cable, W.C. Koehler and E.O. Wollan, Phys. Rev. A 136 (1964) 240.
[30] R. Pott and R. Schefzyk, J. Phys. E – Sci. Instrum. 16 (1983) 444.